

Effect of Variable-Density and Constant-Density Representations of Flow on Simulating Terrestrial Groundwater Discharge into a Coastal Lagoon

Wissam Al-Taliby^{1*}, Hadeel Dekhn²

¹ Department of Environmental Engineering, College of Engineering, University of Babylon, Babylon 51001, Iraq

² Ministry of Construction, Housing, Municipalities and Public Works, Soil Investigation Section, Construction Laboratories, Babylon 51001, Iraq

* Corresponding author's e-mail: waltaliby2011@my.fit.edu

ABSTRACT

Terrestrial groundwater discharge (TGWD) can be an important pathway for pollutants into coastal water bodies. Thus, a reliable way to quantify it is essential for efficient coastal management practices. This study evaluated the feasibility of using constant-density models for estimating TGWD amounts into the Indian River Lagoon, which is a variable-density estuarine environment. Constant-density models were developed using MODFLOW, while variable-density models were developed using SEAWAT. The numerical models were calibrated to match the field measured head data under the lagoon. The amounts of TGWD into the IRL and hydraulic head distributions calculated by the two codes were compared over eight pairs of numerical experiments. Two of those numerical experiments used the calibrated model and field measured conditions, while the rest of them used modified versions of the calibrated models, including variable anisotropy ratio k , variable lagoon salinity L_s , and increased water table elevation by 5%. The results showed that the constant-density model is fairly accurate in estimating TGWD and head distributions at the calibrated k in the range of 1000–20,000 with an error not exceeding 9.4% under the actual measured field conditions. Even when L_s was assumed to increase to ocean salinity value of 1.0, a case that rarely occurs in IRL, the calibrated constant-density model's accuracy was not affected substantially. However, the constant-density model failed to represent the physics of the variable-density environment at k values lower than 1000, where the error exceeded 129%. Generally, the accuracy of the constant-density model was found to increase substantially at lower L_s and higher water table elevations.

Keywords: Indian River Lagoon, terrestrial groundwater discharge, variable-density, constant-density

INTRODUCTION

Elevated concentrations of dissolved solids in groundwater that occurs in saline environments generate spatial density gradients that affect the groundwater flow patterns. Those density effects introduce additional complexity to the mathematical and numerical simulation of variable-density groundwater flow compared to constant-density systems [Paniconi et al., 2001]. Submarine groundwater discharge (SGD) [Langevin, 2003; Li et al., 2009] and saltwater intrusion [Lu et al., 2021; Roy and Datta, 2020; Ding et al., 2014;

Chang and Clement, 2018; Lin et al., 2009] are examples of such variable-density flow conditions. SGD is comprised of multiple components; terrestrial groundwater discharge (TGWD), which originates from fresh groundwater recharge that penetrates the aquifer, constitutes one of the most important SGD components as it represents a pathway of land-based pollutants. Numerical modeling of those flow regimes, where flow physics are driven by fluid density, typically incorporates the equations of flow and transport to represent the association between fluid density and salt concentration. SEAWAT [Guo and Langevin,

2002; Langevin et al., 2003; Langevin and Guo, 2006] is one of the numerical codes developed by the U.S. Geological Survey (USGS) for solving the equations of variable-density flow and mass transport by coupling MODFLOW 2000 [Harbaugh et al., 2000] and MT3DMS [Zheng and Wang, 1999]. In the situations where density gradients are small or negligible, a constant-density flow model using MODFLOW may be sufficient to simulate the groundwater flow.

Obviously, variable-density models are more efficient and precise in representing the flow conditions in saline environments compared to constant-density models. However, constant-density scheme may also be a considerable option that groundwater modelers and water resources managers may opt to utilize for modeling variable-density flow systems for several reasons. Extended computational time associated with running variable-density models is probably one of those reasons especially for complex computer models and in the situations where quick and preliminary decision making is needed as well as when high accuracy is not necessary. In such situations, eliminating some key physics for producing faster results may be justifiable. Furthermore, a wide range of geological and physical parameters is usually required for developing and calibrating variable-density models, such as diffusion coefficients and dispersivity, which are rarely available from the field. Therefore, the use of estimated values of those parameters elevates the level of inaccuracy and uncertainty of the model.

Several previous studies have compared constant-density to variable-density solutions of groundwater flow in different large-scale and laboratory-scale saline environments. It was found that constant-density solutions produced similar results to variable-density solutions under certain variable-density conditions. For Instance, Henry problem [Henry, 1964], which is a well-known saltwater intrusion problem, was solved by [Simpson and Clement, 2003] using variable-density and constant density schemes. It was found that constant-density solutions produced quite similar salinity distributions to those obtained by variable-density solutions when the recharge rate was doubled. They also concluded that constant-density solutions failed in producing reliable results under transient conditions. In another investigation that involved Henry problem, [Dentz et al., 2006] also found that constant-density models produced similar results to those obtained from

variable-density solution at higher recharge rates. Constant-density and variable-density solutions of Henry problem conducted by [Al-Taliby and Pandit, 2017] also revealed that anisotropy ratio and freshwater recharge are amongst the most critical parameters that effect the matching between the two solutions. In another investigation, [Arlai and Koch, 2009] compared the two solution schemes in a two-dimensional coastal aquifer of 1000 m by 100 m and they concluded that the predicted Ghyben-Herzberg interface was closely simulated by the variable-density solution and not the constant-density solution. A vertical plane model of a hypothetical coastal aquifer which is larger in domain but similar in boundary condition to Henry problem was developed by [Motz and Sedighi, 2013] and solved by the variable-density method using SEAWAT and constant-density using MODFLOW. Hydraulic heads and fluxes simulated by MODFLOW were found to be comparable to those simulated by SEAWAT on the model's freshwater boundary.

On the basis of the previously described literature, the fluid density gradients in variable-density environments are mostly affected by two parameters: the regional freshwater component recharging the aquifer, and the hydraulic conductivity anisotropy k . Thus, these two parameters are expected to govern the degree of discrepancy between variable-density and constant-density solutions. Furthermore, groundwater salinity is also expected to play a significant role in the density gradients and subsequently, in the accuracy of constant-density solutions.

In this research, the variable-density and constant-density solutions were obtained from calibrated numerical models of a surficial coastal aquifer beneath the Indian River Lagoon (IRL), Florida. The constant-density models were developed using MODFLOW, while the variable-density models were developed using SEAWAT. The models of SEAWAT and MODFLOW were calibrated with similar hydraulic conductivity distribution and the following results were compared and investigated: i) hydraulic head distribution below IRL and ii) amount of TGWD into the IRL. The above-mentioned results were compared under three different modeling conditions including: hydraulic conductivity anisotropy k , IRL salinity L_s , and aquifer water table elevation.

The outcomes of this research deliver some key guidelines to groundwater modelers regarding the worthiness of using constant-density

models in solving the groundwater problems that involve the occurrence of saltwater in the flow system. The paper also presents a quantitative evaluation of the magnitude of error in calculating groundwater seepage using constant-density models in a saltwater environment.

MATERIALS AND METHODS

Study site

The site studied in the current investigation is the Indian River Lagoon (IRL) which is one of three main sublagoons including Banana River Lagoon and Mosquito Lagoon that together constitute the entire Indian River Lagoon System (IRLS) as seen in Figure 1. This estuarine system, which stretches over about 251 km on the Atlantic coast of Florida, is shallow with its average depth not exceeding 2 m. Due to its connectivity to the ocean through natural inlets, the lagoon water is brackish (Fig.1). The IRLS is surrounded by the Barrier Island from the east coastline and the Mainland from the west. The aquifer under the lagoon is unconfined with sand and shells, sandy clay, and clayey geological units. The surficial aquifer is separated from the underlying confined aquifer by marl and clay impervious formation known as Hawthorn formation [Brown et al., 1962]. Within the 3575 km² [Martin et al., 2007] IRLS watershed shown in Figure 1, groundwater seepage into the lagoon comes mainly from the Mainland, while the Barrier Island contributes much lower seepage owing to its narrow area. As shown in Figure 1, the selected study transect is located across the IRL at Brevard County. The transect is directed perpendicular to the lagoon shoreline passing through the Mainland, the IRL, the Barrier Island, and eventually to the coastline.

Field data collection setup

In order to conduct data collection and model development, several single and clusters of on-shore and offshore observation wells and piezometers made of PVC pipes were driven into the aquifer along the selected transect, as shown in Figures 2 and 3.

Several existing surface water points were utilized in addition to the installed observation wells to locate the groundwater divide on the Mainland side. The water table elevations were measured at

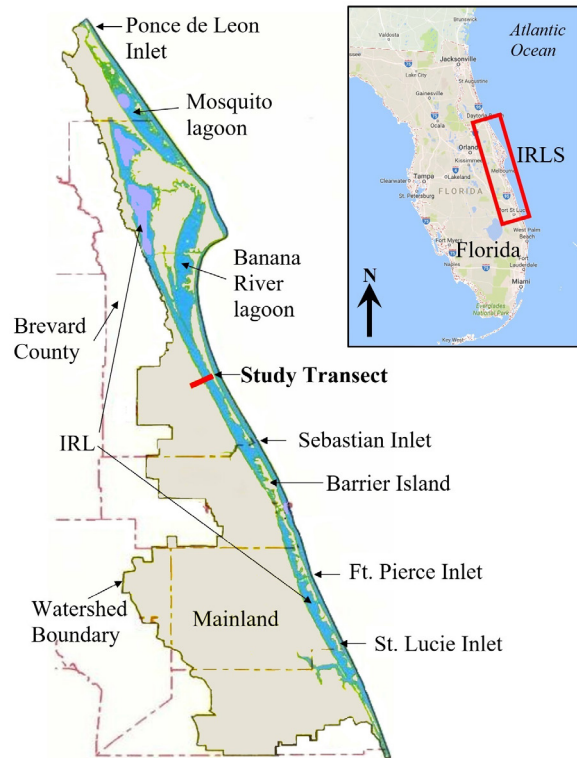


Figure 1. A map of the study area and the location of study transect

those points and wells, and maps of groundwater contours of the surficial aquifer were developed using kriging interpolation (Figure 3). The transect was then located to extend from the established groundwater divide to the ocean. The lagoon bed depth was measured from the west shore to east shore at several locations and the bed shape was established as shown in Figure 4. Clusters of deep and shallow monitoring piezometers were installed at several stations across the transect for collecting groundwater head and salinity measurements under the IRL (Figure 2). The vertical distribution and depths of those observation piezometers are illustrated in Figure 4.

In this research, field data was collected over two different sampling seasons: May and September. Each sampling season took one day to complete. On the day of any sampling season, data collecting included the measurement of groundwater piezometric head and salinity in the offshore stations, the lagoon surface water salinity, and water table elevations in the observation stations located on the Mainland and Barrier Island. The measured water table elevations on the mainland and Barrier Island were fitted into polynomial models of water table profiles to serve as terrestrial boundary conditions. All elevations were converted into National Geodetic Vertical Datum



Figure 2. Extent of the transect and offshore observation stations

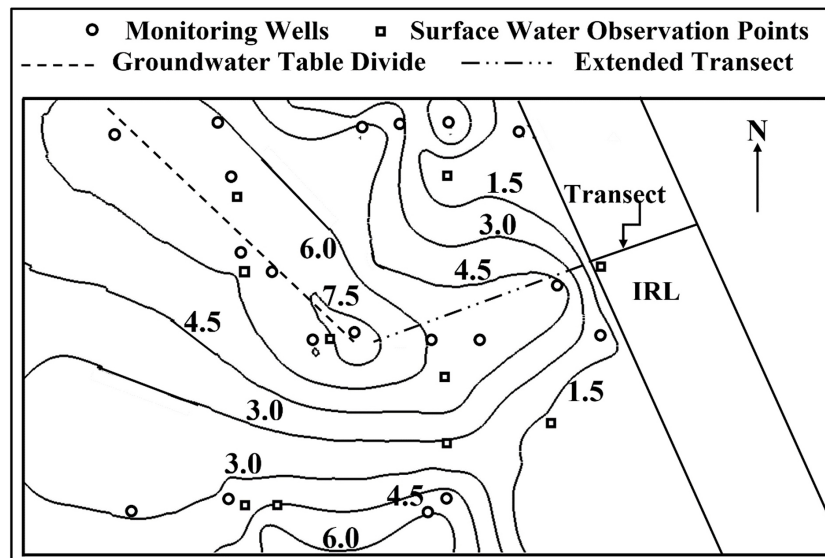


Figure 3. Monitoring locations and groundwater contours (in meter) on the Mainland showing the location of groundwater divide

of 1929 (NGVD29). The measured groundwater elevations at the groundwater divides and lagoon surface water elevation are given in Table 1.

Numerical modeling

Numerical models have been developed using SEAWAT and MODFLOW for the variable-density and constant-density simulations, respectively. Finite difference grid and model domain dimensions are shown in Figure 5.

The model is comprised of a two-dimensional domain with a total horizontal distance of 9.74 km and a total depth of 33.5 m extending down to the confining Hawthorn formation. Finite difference mesh discretization is comprised of 22 layers and 76 columns. Columns vary in

spacing from (15–300 m) and layers are spaced at (0.3–6 m). Both SEAWAT and MODFLOW models are set with identical finite difference mesh discretization.

In terms of boundary conditions, and referring to Figure 5, the MODFLOW and SEAWAT models developed in this research simulated identical boundary conditions for all boundaries except saltwater boundaries (i.e. BC and DE). Constant head boundary type was assigned to boundaries AB and CD that represent terrestrial freshwater input into the model. The values of constant heads were obtained from the polynomial equations developed by statistical regression of the measured head data. The groundwater divide and Hawthorn boundary (AF and FE, respectively) were simulated as No-flow boundaries. In MODFLOW,

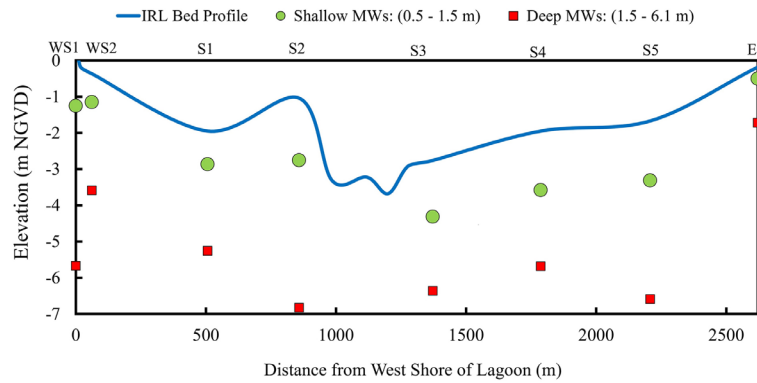


Figure 4. Transect bed shape and locations of shallow and deep observation wells

Table 1. Measured groundwater and IRL surface water elevations

Sampling season	Groundwater divide (m NGVD29)		IRL's water surface (m NGVD29)
	Mainland	Barrier Island	
May	7.518	0.366	0.183
September	8.829	0.591	0.576

constant head values at saltwater boundaries BC and DE, which are IRL and the ocean, respectively, were in the form of equivalent freshwater hydraulic heads obtained from Eq. (1). Conversion of the measured hydraulic head values into equivalent freshwater head values was conducted in the constant-density model to account for density effects. However, SEAWAT automatically performs the conversion of measured heads into equivalent freshwater heads using the specified salt concentrations.

$$h_{fw} = z + \left[\left(1 + \left(\frac{\rho_s - \rho_f}{\rho_f} \right) C \right) (h_s - z) \right] \quad (1)$$

where: h_{fw} is equivalent freshwater hydraulic head,
 z is node elevation from the top of the Hawthorn boundary,
 ρ_s is density of saltwater,
 ρ_f is density of freshwater,
 h_s represents piezometric surface above Hawthorn boundary,
 C is the measured normalized salinity at the boundary.

Numerical models were calibrated to match the measured hydraulic heads observed in May and September below the lagoon (Figure 4). Horizontal hydraulic conductivity K_h was estimated to be 30 m/day by applying Hazen equation [Hazen

1911] on the soil samples collected from the sediments. A summary of model input data used in this study is given in Table 2.

The main calibration parameter was the vertical hydraulic conductivity K_v . Model calibration was accomplished by continuously adjusting zones and values of K_v until a good match was achieved between the observed and modeled head values. The goodness of calibration was evaluated using three statistical measures, including: correlation coefficient, root mean square error (RMSE), and Nash-Sutcliffe Efficiency (NSE) index [Nash and Sutcliffe, 1970]. As shown in Figure 6, a correlation coefficient of 0.97, an RMSE of 0.091, and an NSE of 0.925 are calculated from the calibration results. Those statistics indicate very good calibration.

The ultimate calibrated K_v was in the range of 0.0015 to 0.03 m/day. The majority of model domain had a calibrated K_v value of 0.015 m/day. The corresponding calibrated anisotropy ratio ranged from 1000–20,000 and the predominant value is 2000. The exact calibrated K_v distribution was also used in the constant-density MODFLOW model.

Numerical experiments

A total of eight pairs of numerical experiments were conducted using each of SEAWAT and MODFLOW. The results produced by MODFLOW were compared with those simulated by SEAWAT in each experiment. The details of these experiments are provided in Table 3.

In the first two experiments, the respective May and September boundary conditions and IRL salinity were used to run the models at the calibrated anisotropy ratio to compare the reliability constant-density model under real-world field conditions. Experiments 3 and 4 used the

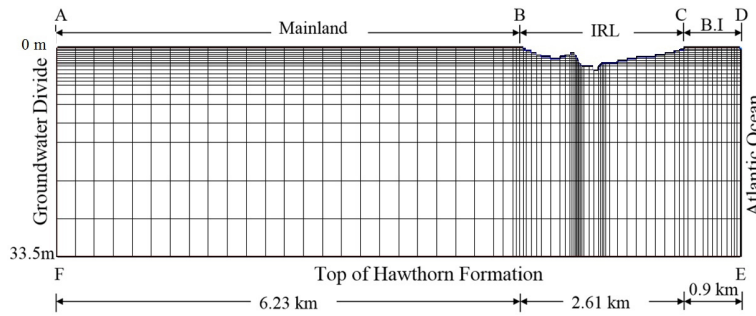


Figure 5. Finite difference grid of IRL models and domain dimensions

Table 2. Model parameters and input data used in the calibrated models

Aquifer parameters	Values
Horizontal conductivity, K_h (m/day)	30
Vertical conductivity, K_v (m/day)	0.0015 to 0.03
Porosity, n	0.3
Specific storage, S_s (m^{-1})	0.00001
Specific yield, S_y	0.01
Longitudinal dispersivity, α_L (m)	30
Transverse dispersivity, α_T (m)	3
Vertical dispersivity, α_v (m)	0.3
Molecular diffusion coefficient, D_m (m^2/d)	0
Lagoon water normalized salinity, S_l	Variable (Table 3)

exact May input data except that the IRL salinity was increased from 0.844 to 0.95 and 1 to study the effect of lagoon salinity on the results. The effect of anisotropy ratio was investigated in experiments 5, 6, and 7 by changing k from the May calibrated conditions to 100,000, 100, and 10, respectively with keeping the other May conditions

the same. Experiment 8 was conducted to study the effect of increasing freshwater recharge observed in May by 5%.

RESULTS AND DISCUSSION

Inspecting the results given in Table 3, constant-density model simulated TGWD with 9.4% error compared to the values simulated by the variable-density model in experiment 1. The accuracy of the constant-density model increased in experiment 2 by a factor of 3 with only 3.2% error because of the lower lagoon salinity (Table 3) and higher groundwater levels (Table 2). These results give the impression that constant-density models can replicate variable-density results to a reasonable level under real conditions especially under lower saline conditions and higher freshwater recharge. The groundwater head distributions predicted by constant-density and variable-density

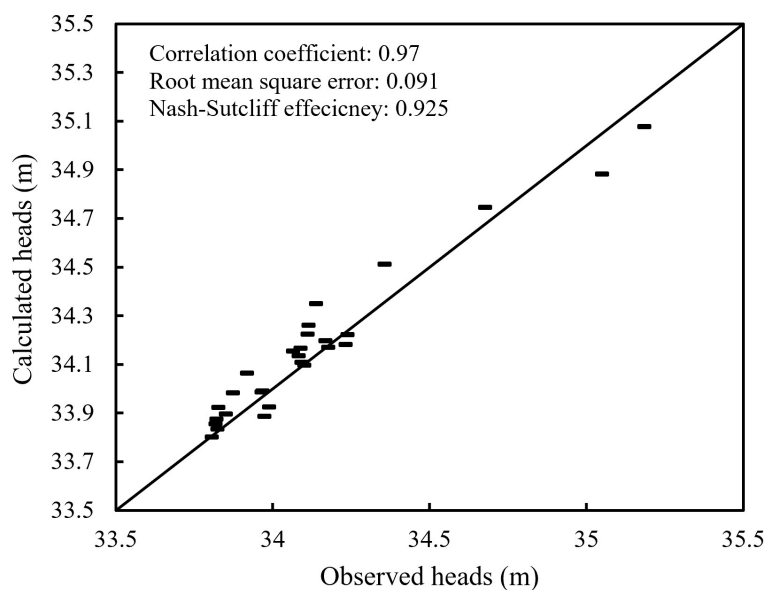


Figure 6. A scatter plot showing field head data observed in May and September versus SEAWAT simulated head values and statistics of calibration goodness

Table 3. Conditions and results of numerical experiments

Exp. no.	Anisotropy ratio k	IRL salinity S_L	Boundary conditions	TGWD received in IRL		
				SEAWAT (m ³ /day/m)	MODFLOW (m ³ /day/m)	Error (%)
1	1000–20,000	0.844	May	1.79×10^{-4}	1.96×10^{-4}	9.4
2	1000–20,000	0.306	September	1.82×10^{-4}	1.88×10^{-4}	3.2
3	1000–20,000	0.950	May	1.76×10^{-4}	1.95×10^{-4}	10.7
4	1000–20,000	1.000	May	1.75×10^{-4}	1.95×10^{-4}	11.3
5	100,000	0.900	May	4.12×10^{-5}	4.34×10^{-5}	5.3
6	100	0.900	May	2.59×10^{-4}	3.57×10^{-4}	38.2
7	10	0.900	May	2.19×10^{-4}	5.02×10^{-4}	129.4
8	1000–20,000	0.844	(a)*	4.73×10^{-4}	4.95×10^{-4}	4.5

models for experiments 1 and 2 are compared in Figures 7 and 8, respectively. The constant-density approach reproduced the head distribution calculated by variable-density model into a remarkable level. The effect of lower lagoon salinity and higher groundwater levels in experiment 2 in improving the accuracy can also be seen when Figure 8 is compared with Figure 7. The density effects are obvious in the simulated head distributions (Figures 7 and 8) on the ocean boundary.

Experiments 3 and 4 used the same k distribution and boundary conditions as experiment 1, except that lagoon salinity was increased to 0.95 in experiment 3 and 1.00 in experiment 4. The results of these two pairs of numerical runs confirm that the discrepancy between constant-density and variable-density models in predicting the amount of TGWD into the lagoon increases with increasing lagoon salinity. However, increased IRL salinity does not seem to significantly affect the amount of TGWD predicted by either method.

This can be seen from Table 3 where TGWD predicted by SEAWAT in experiment 1 which is 1.79×10^{-4} m³/day/m decreased very slightly to only 1.76×10^{-4} m³/day/m and 1.75×10^{-4} m³/day/m in experiments 3 and 4, respectively. The MODFLOW results of these two experiments showed similar behavior. It also can be seen that the amounts of TGWD predicted by either method are still lower than those simulated in experiment 2 of September sampling season. Thus, it can be inferred that the amounts of TGWD are governed by hydraulic gradient between the model boundaries and lagoon water level. It is also worth mentioning that increasing IRL salinity in experiments 3 and 4 did not produce much different head distributions from those presented in Figures 7 and 8.

Increasing k value to 100,000 in experiment 5 compared to experiment 1 seems to reduce the error of MODFLOW prediction of TGWD to 5.3%. However, decreasing k to 100 and 10 in

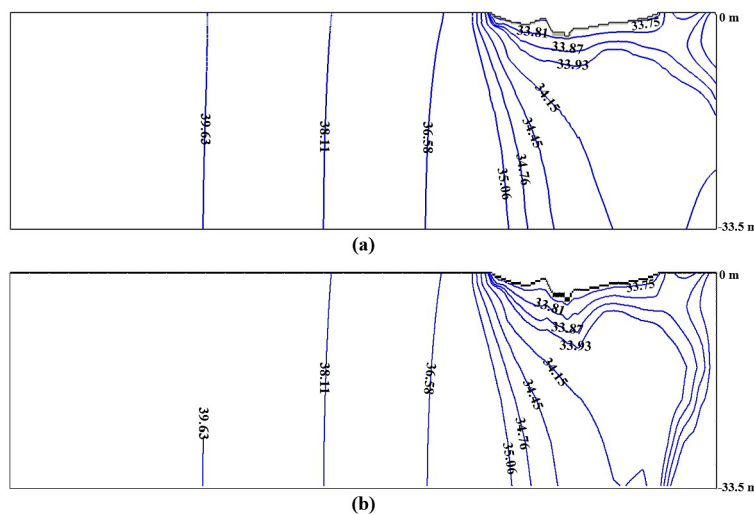


Figure 7. Groundwater head distributions simulated in experiment 1 using (a) constant-density MODFLOW and (b) variable-density SEAWAT

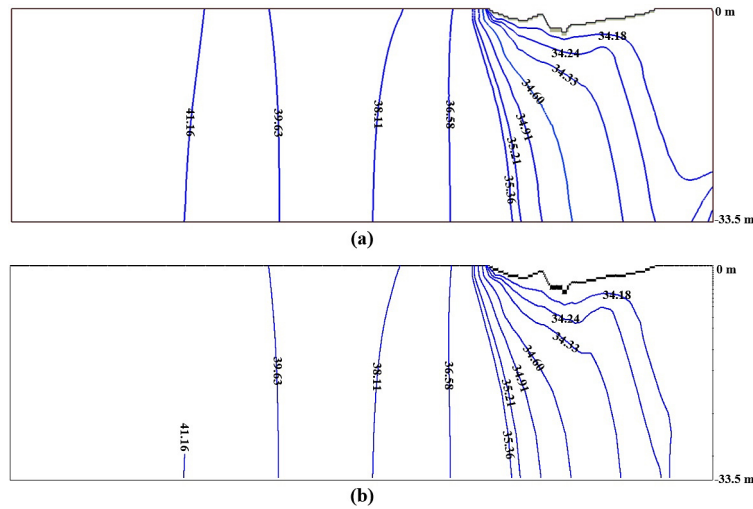


Figure 8. Groundwater head distributions simulated in experiment 2 using (a) constant-density MODFLOW and (b) variable-density SEAWAT

experiments 6 and 7, respectively, caused the error to significantly increase up to 129.4%. This is because decreasing k is equivalent to increasing K_v which results in increased density effects due to the vertical encroachment of lagoon salinity into the aquifer and therefore, the density effects predominate over the advective forces. Figure 9 shows how MODFLOW fails to reproduce the hydraulic head distribution predicted by SEAWAT when k is increased to 100.

The error of constant-density model in calculating TGWD is lowered to 4.5% which is equivalent to 50% improvement compared to experiment 1 when the groundwater levels were increased by just 5% in experiment 8 (Table 3). This improved accuracy of the constant-density

model is also seen in the predicted head distributions shown in Figure 10.

Despite the wake of increasing computational abilities of modern high-speed computers, extended run times, especially for complex three-dimensional groundwater models such as regional models have always represented a challenge. In this study, each of the numerical experiments ran in SEAWAT required 564 seconds to finish. However, it only required 0.07 seconds for MODFLOW to obtain the solutions. Running refined mesh experiments was also conducted in this research and it was found that constant-density models can run faster than variable-density models by a factor of 7000 and still produce similar results under moderately saline conditions.

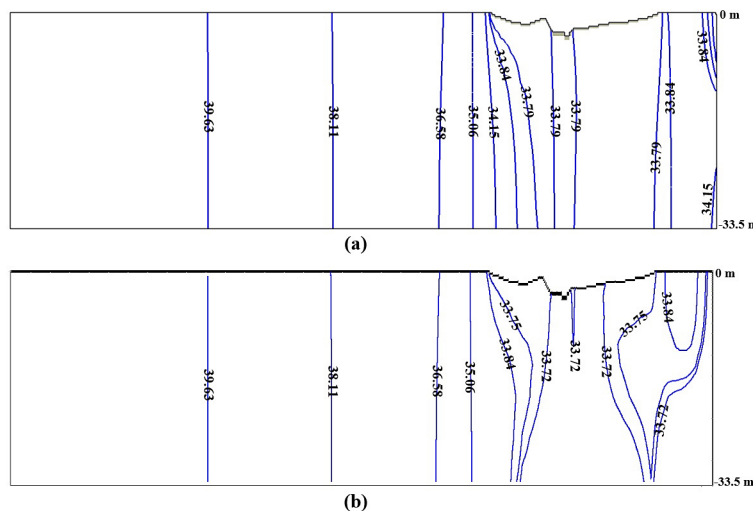


Figure 9. Groundwater head distributions simulated in experiment 6 using (a) constant-density MODFLOW and (b) variable-density SEAWAT with $k = 100$

11. Langevin C.D. 2003. Simulation of submarine ground water discharge to a marine estuary: Biscayne Bay, Florida. *Groundwater*, 41(6), 758–771.
12. Langevin C.D., Guo W. 2006. MODFLOW/MT3DMS-based simulation of variable density ground water flow and transport. *Groundwater*, 44(3), 339–351.
13. Langevin C.D., Shoemaker W.B., Guo W. 2003. MODFLOW-2000, the U.S. Geological Survey modular ground-water model: Documentation of the SEAWAT-2000 version with the variable-density flow processes (VDF) and the integrated MT3DMS Transport Processes (IMT). USGS Open-File Rep. 03–426, U.S. Geological Survey, Tallahassee, FL.
14. Li X., Hu B.X., Burnett W.C., Santos I.R., Chanton J.P. 2009. Submarine ground water discharge driven by tidal pumping in a heterogeneous aquifer. *Groundwater* 47(4), 558–568.
15. Lin J., Snodsmith J.B., Zheng C., Wu J. 2009. A modeling study of seawater intrusion in Alabama Gulf Coast, USA. *Environmental Geology*, 57, 119–130.
16. Lu P., Lin K., Xu C., Lan T., Liu Z., He Y. 2021. An integrated framework of input determination for ensemble forecasts of monthly estuarine saltwater intrusion. *Journal of Hydrology*, 598.
17. Martin J.B., Cable J.E., Smith C., Roy M., Cherrier J. 2007. Magnitudes of submarine groundwater discharge from marine and terrestrial sources: Indian River Lagoon, Florida. *Water Resources Research*, 43(5), W05440.
18. Motz L., Sedighi A. 2013. Saltwater intrusion and recirculation of seawater at a coastal boundary. *Journal of Hydrologic Engineering*, 18(1), 10–18.
19. Nash J.E., Sutcliffe J.V. 1970. River flow forecasting through conceptual models part I – A discussion of principles. *Journal of Hydrology*, 10(3), 282–290.
20. Paniconi C., Khlaifi I., Lecca G., Giacomelli A., Tarhouni J. 2001. A modelling study of seawater intrusion in the Korba Coastal Plain, Tunisia. *Physics and Chemistry of the Earth, Part B: Hydrology, Oceans and Atmosphere*, 26(4), 345–351.
21. Roy D.K., Datta B. 2020. Saltwater intrusion prediction in coastal aquifers utilizing a weighted-average heterogeneous ensemble of prediction models based on Dempster-Shafer theory of evidence. *Hydrological Sciences Journal*, 65(9), 1555–1567.
22. Simpson M.J., Clement T.P. 2003. Theoretical analysis of the worthiness of Henry and Elder problems as benchmarks of density-dependent groundwater flow models. *Advances in Water Resources*, 26(1), 17–31.
23. Zheng C., Wang P. 1999. MT3DMS- a modular three-dimensional multispecies transport model for simulation of advection, dispersion, and chemical reaction of contaminants in ground-water systems: Documentation and user's guide. Jacksonville, Florida. Contact Report SERDP-99–1, U.S. Army Corps of Engineers.